Theriologia Ukrainica, **26**: 159–166 (2023)
p-ISSN 2616-7379 • e-ISSN 2617-1120
DOI: 10.53452/TU2614

NON-INVASIVE (GEORADAR) INVESTIGATION OF GROUNDHOG (*MARMOTA MONAX*) BURROWS, PENNSYLVANIA, USA

Ilya Buynevich

Key words

bioturbation, georadar, tunnel, slope

doi

http://doi.org/10.53452/TU2614

Article info

submitted 29.07.2023
revised 26.11.2023
accepted 30.12.2023

Language

English, Ukrainian summary

Affiliations

Temple University (Philadelphia, USA)

Correspondence

Ilya V. Buynevich; Department of Earth and Environmental Science, Temple University; 1901 N 13th Street, Philadelphia 19122, USA;
Email: coast@temple.edu;
orcid: 0000-0002-3840-0208

Abstract

Zoogenic impact plays a critical role in stream processes, especially bank stability and resulting channel dynamics. This study focuses on bioturbation by groundhogs (*Marmota monax*) along the riparian zone of Mill Creek (Bucks County, Pennsylvania, USA). Several complexes comprising at least 32 active burrows (average diameter: 25.9 cm) were geolocated, with morphometric measurements obtained at selected sites. Two networks were imaged using high-frequency 800 MHz ground-penetrating radar (GPR) and included: 1) a grid of parallel 3-m-long transects on the south bank, and 2) an 11-m-long profile on the north bank. Post-processed electromagnetic signal traces (A-scans) comprising 2D radargrams (B-scans) revealed voids as reverse-polarity anomalies (hollow inclined shafts and tunnels), allowing for a general assessment of burrow depth and orientation. At the southern cutbank site, a large burrow had an entrance diameter of 0.3 m and a westerly dip. A sloping tunnel section was detected at ~0.5 m depth, based on the geometry of point-source (transverse) hyperbolic diffractions corresponding to the roof and a floor 'pull-up'. The second locality traversed three open burrow entrances adjacent to large tree roots. This survey along a tributary channel shows multiple hyperbolics below adjacent openings, with the latter showing the characteristic signal 'breakout'. GPR data show hyperbolic signatures ~0.3–0.4 m below the ground surface. Along this transect, burrowing activity appears to increase with proximity to the northern bank of Mill Creek. An example of a depth slice (bedding-plane view) from a nearby riverbank demonstrates the potential for 3D visualization (C-scans) of burrow networks using a grid of closely spaced GPR profiles. Groundhog burrows constrain maximum long-term level of the groundwater table and serve as important zoogeomorphic structures in diverse ecotones, including developed landscapes. Abundant evidence of bank slumping, incision, and treefall suggests that burrowing activity likely weakens root systems and enhances groundwater flow, thereby initiating or accelerating geomorphic cascades leading to slope failure.

Cite as

Buynevich, I. 2023. Non-invasive (georadar) investigation of groundhog (*Marmota monax*) burrows, Pennsylvania, USA. *Theriologia Ukrainica*, **26**: 159–166. [In English, with Ukrainian summary]

Неінвазивне (георадарне) дослідження нір бабака лісового (*Marmota monax*), Пенсільванія, США

Ілля Буйневич

Резюме. Зоогенний вплив відіграє вирішальну роль у процесах течії, особливо в стабільності берегів і в результаті динаміці русла. Це дослідження зосереджено на біотурбації бабаків (*Marmota monax*) уздовж прибережної зони струмка Мілл-Крік (округ Бакс, Пенсільванія, USA). Кілька комплексів, що складаються з щонайменше 32 активних нір (середній діаметр: 25,9 см), були геолоковані з морфометричними вимірюваннями, проведеними на вибраних ділянках. Дві мережі нір було візуалізовано за допомогою високочастотного георадару із частотою 800 МГц і включали: 1) сітку паралельних трансектів довжиною 3 м на південному березі та 2) профіль довжиною 11 м на північному березі струмка. Оброблені сліди електромагнітного сигналу (A-скани), що містять 2D радарграми (B-скани), виявили порожнини як аномалії зворотної полярності (похилі шахти та тунелі), дозволяючи загальну оцінку глибини та орієнтації нори. На південній ділянці, велика нора мала діаметр входу 0,3 м і західне падіння. Похилий сегмент тунелю було виявлено на глибині ~0,5 м на основі геометрії точкових (поперечних) гіперболічних дифракцій, що відповідають даху та «підтягуванню» підлоги. Друге місце проходило через три відкриті входи в нори, що примикають до великих коренів дерев. Цей огляд уздовж каналу притоки показує кілька гіперболічних зображень під сусідніми отворами, причому останні демонструють характерний сигнал «прорива». Дані георадара показують гіперболічні сліди ~0,3-0,4 м під поверхнею землі. Уздовж цього розрізу активність риття зростає з наближенням до північного берега Мілл-Крік. Приклад глибинного зрізу (вид площини настилу) з сусіднього берега річки демонструє потенціал 3D-візуалізації (C-скан) мережі нір за допомогою близько розташованої сітки профілів георадарара. Нори лісового бабака обмежують максимальний довгостроковий рівень ґрунтових вод і служать важливими зоогеоморфними структурами в різноманітних екотонах, включаючи антропогенні ландшафти. Численні докази опускання берегів, врізання та падіння дерев, свідчать про те, що діяльність землєроїв, ймовірно, послаблює кореневу систему та посилює потік ґрунтових вод, тим самим ініціюючи або прискорюючи геоморфологічні каскади, що призводять до руйнування схилів.

Ключові слова: біотурбація, георадар, тунель, схил.

Introduction

Semi-fossorial mammals have been shown as important landscape engineers [Butler 1995], an impact with a potentially rich fossil record [Voorhies 1975; Gobetz 2006; Hasiotis *et al.* 2007]. Groundhog or woodchuck (*Marmota monax*) is one of the most prolific burrowers, which often extend their habitat into anthropogenically altered landscapes [Armitage 2003]. Whereas field-intensive excavation, trenching, and casting methods have been used to study burrow networks of smaller animals, large (diameter >20 cm) structures are extremely challenging to map, especially if abandoned or masked by infilling burrows [Voorhies 1975; Reichman & Smith 1990; Cortez *et al.* 2013; *Buynevich et al.* 2014; Kopcznski *et al.* 2017].

To address this, recent advances in rapid, continuous subsurface imaging, such as ground-penetrating radar (GPR or georadar) are being increasingly applied to identify and map large bioturbation structures [Stott 1996; Buynevich, 2011; Kinlaw & Grasmueck 2012; Swinbourne *et al.* 2014; Buynevich, 2023a]. Natural and man-made river embankments, dikes, and levees have received recent attention from detailed GPR-aided monitoring, [Biavati *et al.* 2008; Di Prinzio *et al.* 2010; Chlaib *et al.* 2014; Tanajewski & Bakuła 2016], however little research has focused direct impact of bioturbation on slope stability [Nichol *et al.* 2003; Buynevich *et al.* 2018; Sherrod *et al.* 2019].

This study addresses the zoogeomorphic aspect of bioturbation by combining geophysical imaging and field investigation of groundhog burrow networks along fluvial terraces of south-east Pennsylvania, USA (Fig. 1). The aims of this study are to: 1) demonstrate the viability of high-frequency georadar for imaging shallow burrows of *M. monax*, and 2) to highlight the importance of burrowing activity as an integral part of biogeomorphic cascades in forested riparian settings.

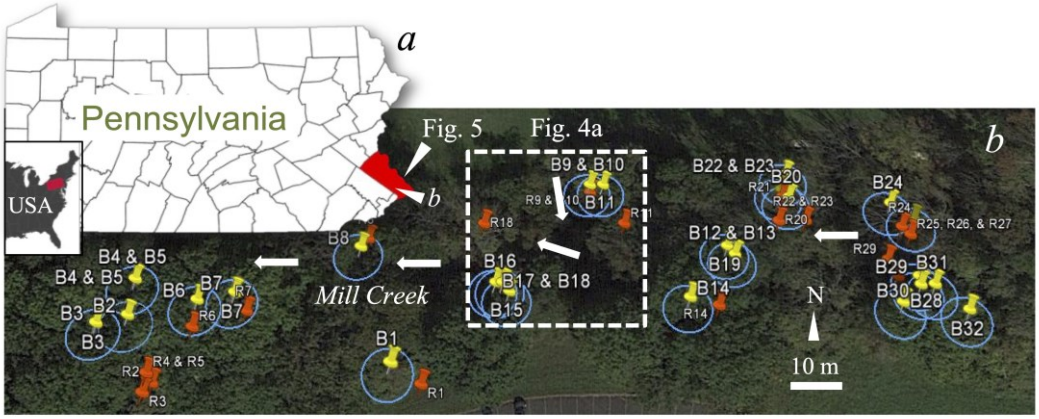

Fig. 1. Location of the study area: (*a*) Bucks County, Pennsylvania, USA. The main Mill Creek site (Fig. 1b) and Delaware River site (Fig. 5) are shown by white arrows; (*b*) Mill Creek site with geolocated active burrows (B— yellow labels). Some clustering is visible (circle: 5 m radius from an opening). Red labels (R) represent closest bank of the Mill Creek (white arrows show flow to the west) (GoogleEarth™).

Рис. 1. Розташування території дослідження: (а) округ Бакс, штат Пенсільванія, США. Головне місце Мілл Крік (Рис. 1b) і ділянка на річці Делавер (Рис. 5) показано білими стрілками; (b) Ділянка Мілл Крік із геолокованими активними норами (B — жовті мітки). Видно деяке скупчення (коло: радіус 5 м від отвору). Червоні мітки (R) позначають найближчий берег струмка (білі стрілки показують течію на захід) (GoogleEarth™).

Materials and Methods

Field surveys conducted along a section of Mill Creek (aka Mill Run, Pennsylvania) between 2017–2019 included photography, geolocation (digital hand-held Garmin GPS), and measurements of active burrow entrances (diameter, minimum achievable depth, and dip azimuth). Geophysical surveys utilised ground-penetrating radar (GPR or georadar) that uses electromagnetic (EM) impulses for rapid continuous imaging of the subsurface [for methodology and post-processing protocols see: Di Prinzio *et al.* 2010; Chlaib *et al.* 2014; Buynevich *et al.* 2014]. High-resolution geophysical images (radargrams) were collected using a digital MALÅ Geoscience system with a shielded 800 MHz monostatic antenna (Fig. 2a). Due to a trade-off between signal penetration and vertical resolution (discrimination between two closely spaced interfaces), this high-frequency setup was most suitable for the present study. Based on empirical data, measured target (burrow) depth, as well as hyperbola fitting during and following the surveys, the EM signal velocity of 8 cm/ns is used for damp organic, clay-rich soils at the study site. The vertical separation between stacked diffractions can be used to estimate the height (diameter) of the void. The along-ground distance along survey lines was provided by the odometer wheel attached to the antenna (Fig. 2a).

In radargrams, a series of wiggle traces (A-scans) are stacked to produce a continuous 2D profile (B-scan; Fig. 2b). Due to cone-shaped transmitted signal geometry, buried three-dimensional objects (point-source reflections) exhibit a typical hyperbolic (high-amplitude diffraction) response (Fig. 2b). The apex of the hyperbola represents the actual position of the buried target and air-filled cavities produce a characteristic ‘pull up’ (early signal arrival) of the floor due to higher velocity in air than in sediment [Fig. 4; Nichol *et al.* 2003]. Traverses directly over burrow openings result in early direct signal arrival (sharp pull up or ‘breakout’), which extends through a gap in ground-wave reflection. In contrast, a saturated burrow-fill or a live animal will produce a reduction in signal velocity. The shape (tightness) of the diffraction is a function of target size and EM wave velocity of the overlying layer, both of which cause broadening in limb separation.

Besides signal velocity, its polarity pattern can be used to assess subsurface changes [Chlaib *et al.* 2014; Buynevich *et al.* 2021]. As a high-amplitude interface response in a given A-scan is compared to the air-ground interface return (velocity reduction), the polarity pattern (red/blue [+/–] sequence) would be either the same (normal) or opposite (reversed; Fig. 2b).

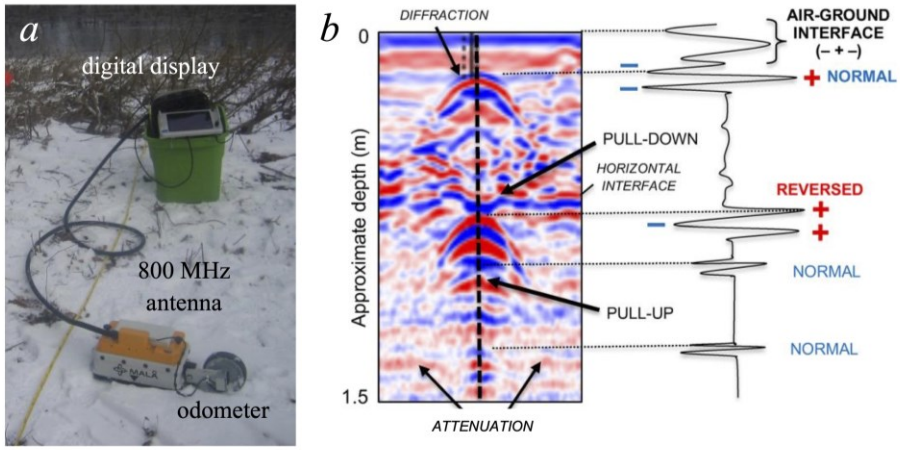

Fig. 2. Subsurface imaging method: (*a*) An 800 MHz georadar antenna, with an odometer wheel providing along-ground distance; (*b*) 2D radargram (B-scan) contains several vertically stacked hyperbolic diffractions (convex anomalies). A synthetic A-scan wiggle-trace at right shows a polarity pattern of the air–ground interface (– + –) and the anomalies below with a similar response that are considered normal (also note the signal pull-down below resulting from a decrease in velocity). A strong reflection in the middle has a reversed polarity (+ — +), which is common for an air-filled void, as corroborated by a signal pull-up (velocity increase) just below. The low velocity through the upper anomaly results in a tighter diffraction of the upper interface of the middle target (e.g. burrow roof; from [Buynevich *et al.* 2021]).

Рис. 2. Метод отримання зображень під поверхнею: (а) Антена георадара 800 МГц з колесом одометра, що визначає відстань уздовж землі; (b) 2D радарограмма (B-скан) містить кілька вертикально розташованих гіперболічних дифракцій (опуклих аномалій). Синтетичний A-скан справа показує полярність контакту «повітря-земля» (– + –) та аномалії нижче з подібним відгуком, які вважаються нормальними (також зверніть увагу на спад сигналу внизу в результаті зменшення у швидкості). Потужне відображення в середині має зворотну полярність (+ — +), що є звичайним для заповненої повітрям порожнечі та підтверджується підтягуванням сигналу (збільшення швидкості) трохи нижче. Повільна швидкість через верхню аномалію призводить до щільнішої дифракції верхньої межі розділу середньої цілі (напр., дах нори; за: [Buynevich *et al.* 2021]).

For instance, if a subsurface interface has normal polarity, it is associated with a signal deceleration (e.g. increased moisture content, live animal, etc.). Polarity reversal would indicate a velocity increase (e.g. empty or air-dominated void; Fig. 2b). Raw GPR images were post-processed with a RadExplorer v.1.41 software package and are presented as two-dimensional images (B-scans). The post-processing algorithm followed a standard protocol [see: Di Prinzio *et al.* 2010; Buynevich *et al.* 2014]. No surface normalization was applied due to negligible topographic variations over short survey distances.

Results

For 32 mapped burrows, entrance diameters varied between 10–45 cm, with a mean of 25.9 cm. The majority (>80%) of the burrows were within 5 m of streambank, with the remainder between 10–20 m. Many creek slope sections adjacent to burrows show extensive undercutting, root exposures, and treefall (Fig. 3b).

Geophysical images both across and along dipping entrance tunnels contain hyperbolic diffractions (point-source reflections). At the southern bank site, a burrow within 1.5 m of the cutbank had an entrance diameter of 0.3 m and a westerly dip angle of ~40°, roughly parallel to the stream flow direction. It was imaged both along and across the trend of an inclined entrance tunnel (Fig. 4a). A 3-m-long transverse image presented here (Line 191) reveals a clear double-diffraction feature at a depth of ~0.5 m below the topsoil, the deeper interface being a ‘pull-up’ (see Fig. 4b). The top high-amplitude reflections has a reversed polarity pattern (e.g. sequence of red/blue [+/–] lines; see Fig. 2b), whereas the polarity pattern of the bottom return is normal (Fig. 4b).

Fig. 3. Zoogeomorphic impact: (*a*) Multiple entrances along the north (right) bank site, with a tributary channel in the distance; (*b*) Eroding south (left) creek bank near an active groundhog burrow is characterised by exposed roots (small arrows) and fallen trees (large arrows).

Рис. 3. Зоогеоморфологічний вплив: (а) Декілька входів уздовж північного (правого) берега, з притоковим каналом на відстані; (b) Ерозія південного (лівого) берега струмка поблизу активної нори бабака характеризується відкритими корінням (маленькі стрілки) і поваленими деревами (великі стрілки).

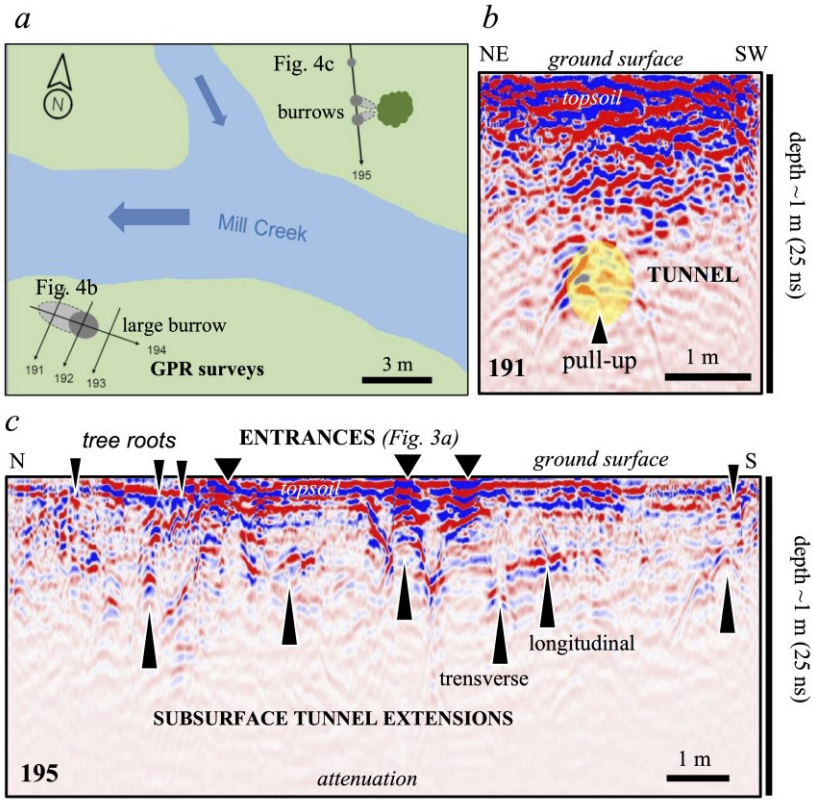

Fig. 4. Subsurface images (2D radargrams) of groundhog burrows: (*a*) Layout of geophysical surveys; (*b*) Image across a large burrow entrance along the south bank (yellow oval). The two-way travel time in nanoseconds (ns) is used to calculate approximate depth; (*c*) GPR transect across several openings at north bank site. See Fig. 1b for site location.

Рис. 4. Підповерхневі зображення (2D радарграми) нір бабака лісового: (*a*) Схема геофізичних досліджень; (*b*) Зображення через великий вхід у нору вздовж південного берега (жовтий овал). Час подорожі в наносекундах (ns) використовується для розрахунку приблизної глибини; (*c*) Георадарний профіль через кілька отворів на північному березі. Дивіться рис. 1b для розташування ділянки.

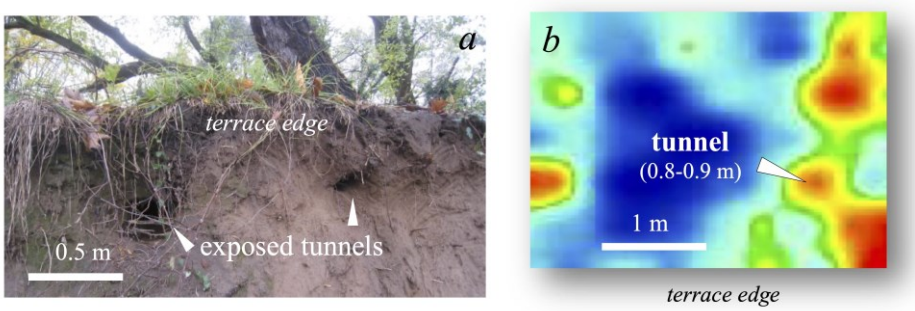

Fig. 5. Depth slice: (a) Large burrows exposed along the western bluff face of Delaware River. A 3D survey grid was collected on the terrace just beyond the edge; (*b*) Horizontal 3x3 m depth surface (z-slice) of shallow burrow tunnels below the river terrace represents a bedding-plane view at 0.8–0.9 m interval. Hot (red/yellow) colors represent high-amplitude anomalies corresponding to extensions of exposed burrows shown in Fig. 5a. See Fig. 1a for site location.

Рис. 5. Зріз глибини: (*a*) Великі нори, відкриті вздовж західного обриву річки Делавер. Сітка 3Dьогляду була зібрана на терасі відразу за краєм; (*b*) Горизонтальна поверхня глибиною 3x3 м (z-зріз) неглибоких тунелів під терасою представляє вигляд площини настилу з інтервалом 0,8–0,9 м. Гарячі (червоні/жовті) кольори представляють високоамплітудні аномалії, що відповідають продовженням відкритих нір, показаних на рис. 5a. Розташування ділянки див. на рис. 1a.

At the northern site, just east (upstream) of a small tributary, an 11-m-long profile traversed several burrows (Line 195; Fig. 4a). In the middle of the transect, imaging of the openings (Fig. 3a) shows a characteristic surface 'breakout' (Fig. 4c; see Methods section above). Similar to the south site, the targets show reverse polarity and there are sections of continuous reflections next to several hyperbolics. At a depth of 0.3–0.4 m, there are multiple targets represented by hyperbolic diffractions with reverse polarity. Small, tight diffractions with normal polarity are present in several sections of the image, are concentrated near the surface and often occur in clusters (Fig. 4c).

Large burrows (likely *M. monax* tunnels exposed by bluff retreat) exposed along the high bank of the Delaware River (Fig. 5a) were imaged using a grid of 3-m-long GPR survey lines, with sufficiently closed line spacing. Ultimately part of a 3D image, a depth slice (z-slice) at 0.8-0.9 m below the terrace surface is presented here (Fig. 5b). High-amplitude reflections in this orientation correspond to subsurface voids that can be correlated with exposed openings.

Discussion

The results of this study show good viability of GPR to image large burrows even in relatively mud-rich substrates. All burrows at Mill Creek were excavated by *Marmota monax*, some of which were observed near entrances during field visits. The high-amplitude diffractions correspond to subsurface extensions of active burrow tunnels and chambers (depth: 0.3–0.5 m; Figs 4*b*–*c*), with a characteristic 'pull-up' of the burrow floor due to high EM wave velocity through air. Sections of continuous reflections adjacent to several point-source hyperbolics are likely (near-) longitudinal tunnel (or chamber) segments (Fig. 4*c*).

The polarity reversal representing the tunnel roof is consistent with sediment-air transition, compared to normal polarity of the floor (air-to-sediment). The subvertical portions (shafts) are not common in groundhog burrows and would produce signal interference [Buynevich *et al.* 2014]. Numerous tight hyperbolas near the surface of the north bank transect are groundtruthed as tree roots (Fig. 4*c*) and may produce complex target patterns when adjacent to burrows.

This research has direct implications for understanding the role of large burrows in weakening regolith integrity, tree root stability, and groundwater pathways (Fig. 3*b* and 5*a*). These processes may initiate or contribute to local geomorphic cascades [Butler 1995; Kinlaw & Grasmueck 2012; Buynevich *et al.* 2018]. Even on low-gradient surfaces, large burrows, especially when masked by vegetation, present danger to walking humans or livestock [Fig. 3*a*; Kopcznski *et al.* 2017; Sherrod

et al. 2019]. Additional information can be obtained from detailed surveys grids, where a series of depth profiles (z-slices) can be used to assess a 3D (C-scan) context of burrow networks (Fig. 5b).

An additional value of identifying, visualising, and mapping burrow networks is their value as indicators of long-term groundwater table position [Buynevich 2003b]. Whereas some burrows have openings above and below water (beaver, desman, etc.), many rodents construct their networks above the water table, making them attractive for other semi-fossorial animals or predators (e.g. foxes). This makes them useful indicators of the maximum long-term water table position [Buynevich *et al.* 2023]. Finally, visualisation of modern burrows helps identify inactive structures, although their recognition may be hampered depending on the fill-to-matrix contrast. Vertebrate burrows are important indicators of terrestrial paleoenvironments [Voorhies 1975; Gobetz 2006; Hasiotis *et al.* 2007; Zonneveld 2016], therefore geophysical imaging can help identify and map paleosol surfaces and bioturbated substrates, especially when non-invasive methodology is required.

Acknowledgements

This research was funded by the College of Science and Technology, Temple University. The author expresses deep gratitude to numerous undergraduate students for their support in the field and to Tyler State Park and Washington Crossing Historic Park for field access.

References

Armitage, K. B. 2003. Marmots: *Marmota monax* and Allies. *In:* Feldhamer, G. A., B. C. Thompson, J. A. Chapman (eds). *Wild Animals of North America Biology, Management, and Conservation*, (2nd ed.). The Johns Hopkins University Press, Baltimore, 188–210.

Biavati G., M. Ghirotti, E. Mazzini, G. Mori, E. Todini. 2008. The use of GPR for the detection of non-homogeneities in the Reno River embankments (north-eastern Italy). *In:* Locat, J., D. Perret, D. Turmel, D. Demers, S. Leroueil (eds.) *Proceedings of the 4th Canadian Conference on Geohazards : From Causes to Management*. Presse de l'Université Laval, Québec, 1–594.

Butler, D. R. 1995. *Zoogeomorphology — Animals as geomorphic agents*. Cambridge University Press, Cambridge, 1–240. CrossRef

Buynevich, I. V. 2011. Buried tracks: ichnological applications of high-frequency georadar. *Ichnos*, **18**: 189–191. CrossRef

Buynevich, I. V. 2023a. Neoichnology of vertebrate traces along the western barrier coast of Ukraine: preservation potential and subsurface visualization. *Geo&Bio*, **24**: 99–105. CrossRef

Buynevich, I. V. 2023b. Biogenic structures as (paleo)hydrologic index points: toward a conceptual framework. *Scientific Research in the Modern World,* Proceedings of the 4th International Scientific and Practical Conference. Perfect Publishing, Toronto, Canada, 220–224.

Buynevich, I. V., H.A. Curran, L. A. Wiest, A. P. K. Bentley, S. V. Kadurin, [et al.]. 2014. Near-surface imaging (GPR) of biogenic structures in siliciclastic, carbonate, and gypsum dunes. *In:* Hembree, D. I., B. F. Platt, J. J. Smith (eds). *Experimental Approaches to Understanding Fossil Organisms: Lessons from the Living.* Springer, Dordrecht, the Netherlands, 405–418. CrossRef

Buynevich, I. V., S. I. Bolysov, A. A. Derkach. 2018. Zoogeomorphic impact along temperate forested fluvial landscapes. *Proceedings of the 36th Geomorphology Conference, Russian Academy of Sciences*, Barnaul, Russia, 75–81. [In Russian]

Buynevich, I. V., T. A. Rothfus, H. A. Curran, H. A., H. A. Thacker, R. Peronace, [et al.]. 2021. High-resolution geophysical imaging of reptile burrows (San Salvador rock iguana, The Bahamas): implications for ichnology and conservation ecology. *Geological Society of London Special Publication*, **522**: 1–9. CrossRef

Buynevich, I. V., S. T. Hasiotis, L. A. Wiest, C. A. Sparacio. 2023. Selected vertebrate and macroinvertebrate zoogenic structures as (paleo-) water-level indicators. *European Scientific Congress,* Proceedings of the 1st International Scientific and Practical Conference. Barca Academy Publishing, Madrid, 219–224.

Chlaib, H. K., H. Mahdi, H. Al-Shukri, M. M. Su, A. Catakli, N. Abd. 2014. Using ground penetrating radar in levee assessment to detect small-scale animal burrows. *Journal of Applied Geophysics*, **103**: 121–131. CrossRef

Cortez, J. D., S. E. Henke, E. Redeker, T. E. Fulbright, R. Riddle, J. Young. 2013. Demonstration of ground-penetrating radar as a useful tool for assessing pocket gopher burrows. *Wildlife Society Bulletin*, **37**: 428–432. CrossRef

Di Prinzio M, M. Bittelli, A. Castellarin, P. R. Pisa. 2010. Application of GPR to the monitoring of river embankments. *Journal of Applied Geophysics,* **7**: 53–61. CrossRef

Gobetz, K. E. 2006. Possible burrows of mylagaulids (Rodentia: Aplodontoidea: Mylagaulidae) from the Late Miocene (Barstovian) Pawnee Creek Formation, northeastern Colorado. *Palaeogeography, Palaeoclimatology, Palaeoecology*, **237**: 119–136. CrossRef

Hasiotis, S. T., B. F. Platt, D. I. Hembree, M. Everhart. 2007. The trace-fossil record of vertebrates. *In:* Miller, W., III (ed.) *Trace Fossils-Concepts, Problems, Prospects*. Elsevier Press, 196–218. CrossRef

Kinlaw, A. E., M. Grasmueck. 2012. Evidence for and geomorphologic consequences of a reptilian ecosystem engineer: the burrowing cascade initiated by the gopher tortoise. *Geomorphology*, **157–158**: 108–121. CrossRef

Kopcznski, K. A., I. V. Buynevich, H. A. Curran, J., Caris, J. E. Nyquist. 2017. Imaging bioturbation in supratidal carbonates: non-invasive field techniques enhance neoichnological and zoogeomorphological research, San Salvador, the Bahamas. *Bollettino della Società Paleontologica Italiana:* **56**: 289–297.

Nichol, D., J. W. Lenham, J. M. Reynolds. 2003. Application of ground-penetrating radar to investigate the effects of badger setts on slope stability at St. Asaph Bypass, North Wales. *Quarterly Journal of Engineering Geology and Hydrogeology*, **36**: 143–153. CrossRef

Reichman, O. J., S. C. Smith. 1990. Burrows and burrowing behavior by mammals. *In:* Genoways, H. H. (ed). *Current*

mammalogy. Plenum Press, New York, 197–244.
Sherrod, L., W. Sauck, E. Simpson, D. D. Jr. Werkema, J. Swiontek. 2019. Case histories of GPR for animal burrow mapping and geometry. *Journal of Environmental and Engineering Geophysics*, **24** (1): 1–17. CrossRef
Stott, P. 1996. Ground-penetrating radar: a technique for investigating the burrow structure of fossorial vertebrates. *Wildlife Research*, 22: 519–530. CrossRef
Swinbourne, M., E. Sparrow, M. Hatch, T. Bowden, D. Taggart. 2014. Using near-surface geophysics to assist with the management of southern hairy-nosed wombats (Lasiorhinus latifrons) in South Australia. *The Leading Edge*, **33** (12): 1346–1362. CrossRef
Tanajewski, D., M. Bakuła. 2016. Application of ground penetrating radar surveys and GPS surveys for monitoring the condition of levees and dykes. *Acta Geophysica*, **64**: 1093–1111. CrossRef
Voorhies, M. R. 1975. Vertebrate burrows. In: Frey RW (ed) The study of trace fossils. *Springer,* New York, 325–350. CrossRef
Zonneveld, J.-P. 2016. Applications of experimental neoichnology to paleobiological and evolutionary problems. *Palaios*, **31**: 275–279. CrossRef